Diffraction by a Structure Composed of Metallic and Dielectric 90° Blocks

Marcello Frongillo, Gianluca Gennarelli, and Giovanni Riccio, *Member*, *IEEE*

***Abstract*— This letter deals with the plane wave diffraction by a composite structure consisting of metallic and lossless dielectric 90° blocks, which are adjacent and share the edge. Such a problem is first tackled in the frequency domain and the related diffraction coefficients are determined by exploiting the uniform asymptotic physical optics approach. The inverse Laplace transform is applied to obtain the time domain counterparts, which can be used to compute the transient diffracted field due to an arbitrary function plane wave.**

***Index Terms*—Propagation, diffraction, wedge, frequency domain, time domain**

I. Introduction

Time consuming and expensive on site measurements or available indoor/outdoor prediction models can be used to estimate the field level at a given location. The Uniform Theory of Diffraction (UTD) is a well-known prediction model able to provide accurate results and useful information for the channel characterization by means of a simple physical representation of the signal propagation. Reflected, transmitted and diffracted rays, and their combinations are used to determine the field in the frequency domain (FD-UTD) as well as in the time domain (TD-UTD) by applying analytical transformations to the FD-UTD solutions.

The diffraction by penetrable wedges in man-made structures assumes a very important role in the propagation analysis and constitutes a challenging problem from the analytic point of view. Representative studies on diffraction by dielectric wedges are reported in [1]-[16]. In particular, frequency domain Uniform Asymptotic Physical Optics (FD-UAPO) solutions have been proposed in [14]-[16] to calculate the diffraction coefficients in the FD-UTD framework. They are expressed in terms of the Geometrical Optics (GO) response of the structure and the standard transition function of the FD-UTD [17]. The FD-UAPO diffracted field can be added to the GO field to guarantee the continuity across the shadow boundaries limiting the existence regions of the GO contributions. Numerical tests proved the efficiency of the FD-UAPO expressions, which are not exact solutions, but they are in closed form and provide reliable results from the engineering viewpoint. Moreover, the approach presented in [18] has been applied to evaluate the TD-UAPO diffraction coefficients associated to plane wave diffraction problems involving dielectric wedges [19]-[21]. The TD-UAPO formulation has the same advantages and limitations of the TD-UTD one. In addition, it retains the FD-UAPO limitations arising from a PO approximation of the electric and magnetic equivalent surface currents located on the internal and external faces of the wedge-shaped dielectric region. Anyway, the TD-UAPO formulation is capable to offer analytical wave solutions to transient diffraction problems involving penetrable dielectric wedges with arbitrary apex angle.

M. Frongillo is with SIRA – Member of the Kathrein Group, via S. Simonetta 26, 20867 Caponago (MB), Italy (e-mail: mfrongillo@sira.mi.it).

G. Gennarelli is with the Institute for Electromagnetic Sensing of the Environment, National Research Council, via Diocleziano 328, 80124 Naples, Italy (e-mail: gennarelli.g@irea.cnr.it).

G. Riccio is with the Department of Information and Electrical Engineering and Applied Mathematics, University of Salerno, via Giovanni Paolo II 132, 84084 Fisciano (SA), Italy (phone: +39 089964285; e-mail: griccio@unisa.it).

The geometry of the considered problem is shown in Fig. 1. One 90° perfect electrically conducting (PEC) block and one 90° dielectric wedge are placed side by side and illuminated by an incident plane wave. The GO field contributions have been determined in [22] and are not reported here. The FD- and TD-UAPO solutions are presented in the following to compute the diffraction coefficients. Preliminary results have been discussed in [22], [23]. Comparisons with full-wave Finite Difference Time Domain (FDTD) data are shown to validate the FD-UAPO solution and to enhance the numerical tests with respect to [22].

II. FD-UAPO Diffraction Coefficients

Figure 1 illustrates the composite structure, which is formed by a 90° PEC block and a 90° dielectric non-magnetic block characterized by the real relative permittivity ε_r. Such a structure is surrounded by free space with impedance ζ_0 and propagation constant k_0. The observation regions Ω and Ω_d coincide with the free space and the dielectric block, respectively. If the *z*-axis of the coordinate system is assumed coincident with the edge shared by the two 90° wedges, the *E*-polarized incident electric field is expressed by $\underline{E}^i = E_0^i \exp(-j\underline{k}^i \cdot \underline{r})\,\hat{z}$, where $\underline{r}$ denotes the position of the observation point *P* and $\underline{k}^i = -k_0(\cos\phi'\hat{x} + \sin\phi'\hat{y})$ is the free-space propagation vector.

According to [14]-[16], the equivalence principle is applied to determine the scattered far-field $\underline{E}^s$ by considering electric ($\underline{J}_s$) and magnetic ($\underline{J}_{ms}$) equivalent surface currents as sources in the radiation integrals related to Ω and Ω_d. A PO approximation is adopted to evaluate such sources.

A. Free-space region Ω

The scattered field in Ω is determined by adding the contributions of the surface currents located on $S_m \cup S_d^+$, where S_m and S_d^+ indicate the external faces of the PEC block and the dielectric one, respectively:

$$\underline{E}_\Omega^s = -jk_0 \iint_{S_d^+} \left[(\underline{\underline{I}} - \hat{R}\hat{R})\zeta_0(\underline{J}_s)_{S_d^+} + (\underline{J}_{ms})_{S_d^+} \times \hat{R} \right] \frac{\exp(-jk_0 R)}{4\pi R}\, \mathrm{d}S_d^+ - jk_0 \iint_{S_m} \left[(\underline{\underline{I}} - \hat{R}\hat{R})\zeta_0(\underline{J}_s)_{S_m} \right] \frac{\exp(-jk_0 R)}{4\pi R}\, \mathrm{d}S_m \,, \tag{1}$$

wherein $\hat{R}$ is the unit vector from the source point $S(\underline{r}')$ to *P* and $R = |\underline{r} - \underline{r}'|$ is the corresponding distance (see Fig. 1). The symbol $\underline{\underline{I}}$ denotes the identity matrix,

$$\zeta_0(\underline{J}_s)_{S_d^+} = (1-\Gamma)E_0^i \sin\phi' \exp(jk_0\rho'\cos\phi')\hat{z} \,, \tag{2}$$

$$(\underline{J}_{ms})_{S_d^+} = -(1+\Gamma)E_0^i \exp(jk_0\rho'\cos\phi')\hat{x} \,, \tag{3}$$

 DOI 10.1109/LAWP.2018.2820738

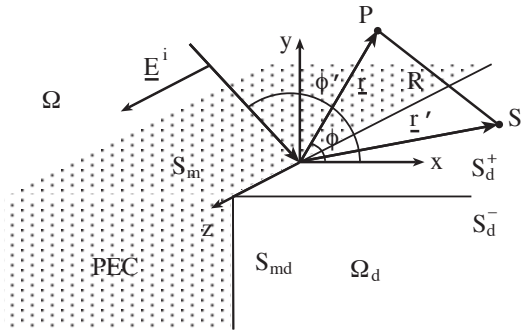

Fig. 1. *E*-polarized plane wave incident on a structure formed by two co-planar adjacent 90° wedges consisting of metallic and dielectric materials.

$$\zeta_0(\underline{J}_s)_{S_m} = 2E_0^i \sin\phi' \exp(jk_0\rho'\cos(\pi-\phi'))\hat{z}\,, \tag{4}$$

with ρ' denoting the distance from *S* to the edge and

$$\Gamma = \frac{\sin\phi' - \sqrt{\varepsilon_r - \cos^2\phi'}}{\sin\phi' + \sqrt{\varepsilon_r - \cos^2\phi'}}\,. \tag{5}$$

The approximation $\hat{R} \cong \hat{s}$ ($\hat{s} = \cos\phi\,\hat{x} + \sin\phi\,\hat{y}$ is the unit vector of the diffraction direction) is adopted in the square brackets of (1). It does not affect the expression of *R* in the phase terms depending on the source point position. This step is permitted to evaluate the UAPO diffracted field [24]. Accordingly, it results:

$$\begin{aligned}
\underline{E}_{\Omega}^{s} &\cong -\frac{jk_0}{4\pi} E_0^i \left[(\underline{\underline{I}} - \hat{s}\hat{s})(1-\Gamma)\sin\phi'\hat{z} - (1+\Gamma)\hat{x}\times\hat{s} \right] \\
&\int_0^{+\infty}\int_{-\infty}^{+\infty} \exp(jk_0\rho'\cos\phi') \frac{\exp(-jk_0|\underline{r} - \underline{r}'(\rho',z')|)}{|\underline{r} - \underline{r}'(\rho',z')|} \mathrm{d}z'\mathrm{d}\rho' \\
&- \frac{jk_0}{4\pi} E_0^i \left[(\underline{\underline{I}} - \hat{s}\hat{s})(2\sin\phi'\hat{z}) \right] \\
&\int_0^{+\infty}\int_{-\infty}^{+\infty} \exp(jk_0\rho'\cos(\pi-\phi')) \frac{\exp(-jk_0|\underline{r} - \underline{r}'(\rho',z')|)}{|\underline{r} - \underline{r}'(\rho',z')|} \mathrm{d}z'\mathrm{d}\rho' \\
&= E_0^i \left[(\underline{\underline{I}} - \hat{s}\hat{s})(1-\Gamma)\sin\phi'\hat{z} - (1+\Gamma)\hat{x}\times\hat{s} \right] I_{S_d^+} \\
&+ E_0^i \left[(\underline{\underline{I}} - \hat{s}\hat{s})(2\sin\phi'\hat{z}) \right] I_{S_m} \\
&= E_0^i \hat{z} \left\{ \left[(1-\Gamma)\sin\phi' - (1+\Gamma)\sin\phi \right] I_{S_d^+} + (2\sin\phi') I_{S_m} \right\} \\
&= E_0^i \hat{z} \left[A_{S_d^+} I_{S_d^+} + A_{S_m} I_{S_m} \right].
\end{aligned} \tag{6}$$

The zeroth order Hankel function of the second kind results from the integration along z' in $I_{S_d^+}$ and I_{S_m}. An integral representation of such a function [25] and the application of the Sommerfeld-Maliuzhinets inversion formula [26] allows one to obtain [24]:

$$I_{S_d^+} = \frac{1}{4\pi j} \int_C \frac{\exp(-jk_0\rho\cos(\alpha-\phi))}{\cos\alpha + \cos\phi'} \mathrm{d}\alpha \tag{7}$$

$$I_{S_m} = \frac{1}{4\pi j} \int_C \frac{\exp(-jk_0\rho\cos(\alpha-(\pi-\phi)))}{\cos\alpha + \cos(\pi-\phi')} \mathrm{d}\alpha \tag{8}$$

where (ρ,ϕ) are the polar co-ordinates of *P* and *C* is the integration path shown in Fig. 2. The integrals in (7) and (8) can be reduced to a typical diffraction integral and evaluated by using the Steepest Descent Method and the Multiplicative Method in the high-frequency approximation. According to [24], the diffraction terms in $I_{S_d^+}$ and I_{S_m} can be so expressed:

$$I_{S_d^+}^d = \frac{\exp(-j\pi/4)}{2\sqrt{2\pi k_0}} \frac{F_t\left(2k_0\rho\cos^2\left((\phi+\phi')/2\right)\right)}{\cos\phi + \cos\phi'} \frac{\exp(-jk_0\rho)}{\sqrt{\rho}} \tag{9}$$

$$I_{S_m}^d = \frac{\exp(-j\pi/4)}{2\sqrt{2\pi k_0}} \frac{F_t\left(2k_0\rho\cos^2\left(\frac{(\pi-\phi)+(\pi-\phi')}{2}\right)\right)}{\cos(\pi-\phi) + \cos(\pi-\phi')} \frac{\exp(-jk_0\rho)}{\sqrt{\rho}} \tag{10}$$

in which $F_t(\cdot)$ is the FD-UTD transition function [17]. Accounting for $I_{S_m}^d = -I_{S_d^+}^d$, the expressions (9) and (10) provide the FD-UAPO diffracted field

$$\underline{E}_{\Omega}^{d} = \left[A_{S_d^+} - A_{S_m} \right] I_{S_d^+}^d E_0^i \hat{z} = D_{\Omega} \frac{\exp(-jk_0\rho)}{\sqrt{\rho}} E_0^i \hat{z} \tag{11}$$

where the diffraction coefficient is given by:

$$D_{\Omega} = -\frac{\exp(-j\pi/4)}{2\sqrt{2\pi k_0}} (1+\Gamma) \frac{\sin\phi + \sin\phi'}{\cos\phi + \cos\phi'} F_t\left(2k_0\rho\cos^2\left(\frac{\phi+\phi'}{2} \right) \right) \tag{12}$$

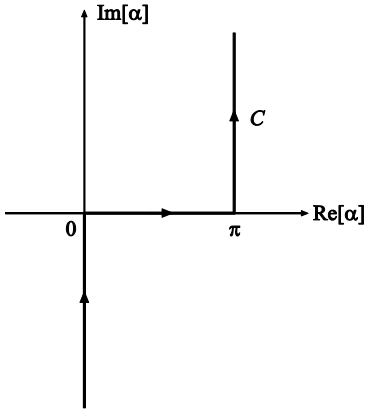

Fig. 2. Integration path *C*.

B. Dielectric region Ω_d

The transmitted field contributes to the evaluation of the PO surface currents on $S_{md} \cup S_d^-$. If $\pi/2 < \phi' < \pi$, the electric PO surface current on S_{md}, which is the PEC face at $x = 0^+$, is not involved in the computation of the FD-UAPO diffraction coefficient D_{Ω_d} since S_{md} is not illuminated by the transmitted field.

If $k_d = k_0\sqrt{\varepsilon_r}$, $U(\phi') = 1$ when $0 < \phi' < \pi/2$ or $U(\phi') = 0$ elsewhere, by applying the analytical procedure used in the previous sub-section it results:

$$D_{\Omega_d} = \frac{\exp(-j\pi/4)}{2\sqrt{2\pi k_d}}\,\tau\left\{\frac{\sin\phi - \sqrt{1-\cos^2\phi'/\varepsilon_r}}{\cos\phi + \cos\phi'/\sqrt{\varepsilon_r}}\right.$$
$$F_t\left(2k_d\rho\cos^2\left(\frac{\phi - \cos^{-1}(\cos\phi'/\sqrt{\varepsilon_r})}{2}\right)\right)$$
$$-\frac{2\cos\phi'/\sqrt{\varepsilon_r}}{\cos(\phi-\pi/2)+\sqrt{1-\cos^2\phi'/\varepsilon_r}}\,U(\phi') \qquad (13)$$
$$\left.F_t\left(2k_d\rho\cos^2\left(\frac{(\phi-\pi/2) - \cos^{-1}(\sqrt{1-\cos^2\phi'/\varepsilon_r})}{2}\right)\right)\right\}$$

with

$$\tau = \frac{2\sin\phi'}{\sin\phi' + \sqrt{\varepsilon_r - \cos^2\phi'}} \qquad (14)$$

All the results shown in this manuscript are relevant to a dielectric block characterized by $\varepsilon_r = 3$. Figure 3 refers to a plane wave impinging at $\phi' = 40°$. The field amplitudes are calculated on a circular path with radius $\rho = 5\lambda_0$ (λ_0 is the free-space wavelength) by assuming $E_0^i = 1$. The GO field possesses two discontinuities at $\phi_{RB} = 140°$ and $\phi_{TRB} = 296°$, which denotes the boundary of the transmission-reflection contribution in Ω_d. The FD-UAPO diffracted field has two peaks at ϕ_{RB} and ϕ_{TRB} as expected and its values allow one to obtain the continuity of the total field. It seems that the proposed solutions work well.

Figures 4 and 5 contain two comparisons with numerical data achieved by means of a FDTD code, which implements the classical Yee algorithm and the total field/scattered field (TF/SF) technique [27]. The incidence direction changes with respect to the first set. A normalized dB scale is used to compare the field levels. The first comparison (see Fig. 4) is relevant to $\phi' = 60°$ and makes evident a very good agreement both in Ω and Ω_d. The latter is reported in Fig. 5 and refers to $\phi' = 140°$. As can be seen, the agreement gradually goes worse in the angular region close S_{md} since the approach neglects the contribution of such a surface, which is not illuminated by the transmitted field through S_d.

III. TD-UAPO Diffraction Coefficients

The TD-UAPO diffraction coefficients d are determined by applying the inverse Laplace transform to the FD-UAPO counterparts under the hypothesis that the dielectric parameters are independent on the frequency. They result so expressed:

A. Free-space region Ω

$$d_\Omega = -\frac{1}{2\sqrt{2\pi}}\left(1+\Gamma\right)\frac{\sin\phi+\sin\phi'}{\cos\phi+\cos\phi'}\,G\left(2\rho\cos^2\left(\frac{\phi+\phi'}{2}\right),t\right) \qquad (15)$$

B. Dielectric region Ω_d

$$d_{\Omega_d} = \frac{1}{2\sqrt{2\pi}}\,\tau\left\{\frac{\sin\phi - \sqrt{1-\cos^2\phi'/\varepsilon_r}}{\cos\phi+\cos\phi'/\sqrt{\varepsilon_r}}\right.$$
$$G\left(2\rho\cos^2\left(\frac{\phi-\cos^{-1}(\cos\phi'/\sqrt{\varepsilon_r})}{2}\right),t\right)$$
$$-\frac{2\cos\phi'/\sqrt{\varepsilon_r}}{\cos(\phi-\pi/2)+\sqrt{1-\cos^2\phi'/\varepsilon_r}}\,U(\phi') \qquad (16)$$
$$\left.G\left(2\rho\cos^2\left(\frac{(\phi-\pi/2)-\cos^{-1}(\sqrt{1-\cos^2\phi'/\varepsilon_r})}{2}\right),t\right)\right\}$$

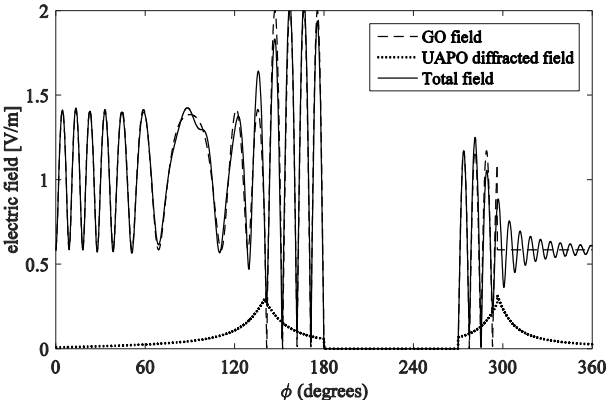

Fig. 3. GO, FD-UAPO and total field amplitudes when $\phi' = 40°$.

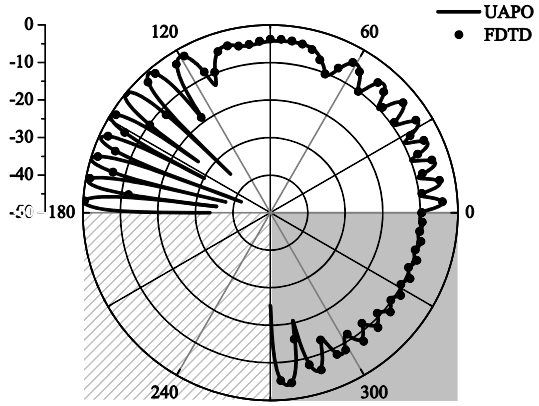

Fig. 4. Comparison between FD-UAPO and FDTD when $\phi' = 60°$.

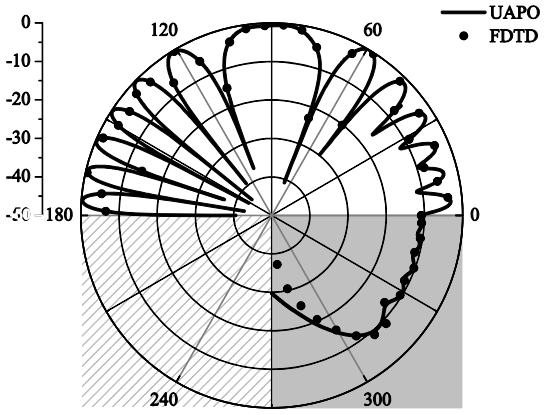

Fig. 5. Comparison between FD-UAPO and FDTD when $\phi' = 140°$.

The expressions (15) and (16) contain the function

$$G(X,t) = X/\sqrt{\pi c t}\,(t + X/c), \tag{17}$$

where c is the light velocity, and can be used to calculate the diffracted field according to [18].

The last two figures show the electric field waveforms arriving at P when a Ricker's function plane wave with central frequency f_c = 1 GHz impacts the structure. The observation time starts when the incident field arrives at the diffraction point. According to $\phi' = 60°$, the arrival time of the transmission waveform in Ω_d is always less than that of the diffraction waveform. The transmission-reflection contribution exists if $\phi < \phi_{TRB}$ (see Fig. 6) and its waveform changes sign with respect to the transmission one as expected.

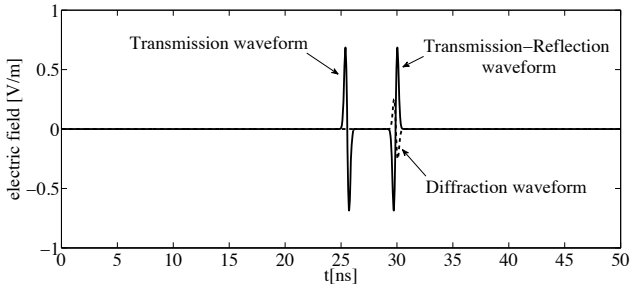

Fig. 6. Electric field waveforms when $\phi' = 60°$ and $P(5\text{m}, 285°)$.

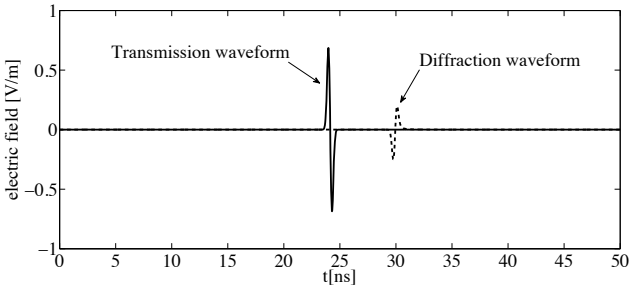

Fig. 7. Electric field waveforms when $\phi' = 60°$ and $P(5\text{m}, 290°)$.

IV. Conclusions

The proposed diffraction coefficients are easy to handle and very efficient from the computational point of view since they contain standard parameters and functions. No special functions and integral equations must be computed by means of numerical techniques. Comparisons with FDTD data assess the effectiveness of the UAPO solutions also in the considered case. On the other hand, the reader must always take into account that inaccuracies arise from the use of the PO approximation, particularly in the shadowed regions.

Note that the analytical procedure can be applied also to a more general structure with non-right angle blocks, but the expressions of the diffraction coefficients will change according to the GO ray-tracing in the dielectric region. The analytical result is not so simple to obtain since multiple reflections and transmissions exist.

References

[1] S. Berntsen, "Diffraction of an electric polarized wave by a dielectric wedge," *SIAM J. Appl. Math.*, vol. 43, pp. 186-211, 1983.

[2] A. D. Rawlins, "Diffraction by, or diffusion into, a penetrable wedge," *Proc. R. Soc. Lond. A*, vol. 455, pp. 2655-2686, 1999.

[3] R. E. Burge *et al.*, "Microwave scattering from dielectric wedges with planar surfaces: a diffraction coefficient based on a physical optics version of GTD," *IEEE Trans. Antennas Propagat.*, vol. 47, pp. 1515-1527, 1999.

[4] J. F. Rouviere, N. Douchin, and P. F. Combes, "Diffraction by lossy dielectric wedges using both heuristic UTD formulations and FDTD," *IEEE Trans. Antennas Propagat.*, vol. 47, pp. 1702-1708, 1999.

[5] C. H. Seo and J. W. Ra, "Plane wave scattering by a lossy dielectric wedge," *Microwave Opt. Technol. Lett.*, vol. 25, 360-363, 2000.

[6] S. Y. Kim, J. W. Ra, and S. Y. Shin, "Diffraction by an arbitrary-angled dielectric wedge: part I–physical optics approximation," *IEEE Trans. Antennas Propagat.*, vol. 39, pp. 1272-1281, 1991.

[7] S. Y. Kim, J. W. Ra, and S. Y. Shin, "Diffraction by an arbitrary-angled dielectric wedge: part II–physical optics approximation," *IEEE Trans. Antennas Propagat.*, vol. 39, pp. 1272-1281, 1991.

[8] P. Bernardi, R. Cicchetti, and O. Testa, "A three-dimensional UTD heuristic diffraction coefficient for complex penetrable wedges," *IEEE Trans. Antennas Propagat*., vol. 50, pp. 217-224, 2002.

[9] M. A. Salem, A. H. Kamel, and A. V. Osipov, "Electromagnetic fields in presence of an infinite dielectric wedge," *Proc. R. Soc. Lond*. A, vol. 462, pp. 2503-2522, 2006.

[10] V. Daniele and G. Lombardi, "The Wiener-Hopf solution of the isotropic penetrable wedge problem: diffraction and total field," *IEEE Trans. Antennas Propagat.*, vol. 59, pp. 3797-3818, 2011.

[11] E. N. Vasilev and V. V. Solodukhov, "Diffraction of electromagnetic waves by a dielectric wedge, " *Radiophysics and Quantum Electronics,* vol. 17, pp. 1161-1169, 1976.

[12] E. N. Vasilev, V. V. Solodukhov, and A. I. Fedorenko, "The Integral Equation Method in the Problem of Electromagnetic Waves Diffraction by Complex Bodies," *Electromagnetics*, vol. 11, 161-182, 1991.

[13] B. Budaev, Diffraction by Wedges. London: Longman Scient, 1995.

[14] G. Gennarelli and G. Riccio, "A uniform asymptotic solution for diffraction by a right-angled dielectric wedge," *IEEE Trans. Antennas Propagat.*, vol. 59, pp. 898-903, 2011.

[15] G. Gennarelli, G. Riccio, "Plane-wave diffraction by an obtuse-angled dielectric wedge," *J. Opt. Soc. Am. A*, vol. 28, pp. 627-632, 2011.

[16] G. Gennarelli, M. Frongillo, and G. Riccio, "High-frequency evaluation of the field inside and outside an acute-angled dielectric wedge," *IEEE Trans. Antennas Propagat.*, vol. 63, pp. 374-378, 2015.

[17] R. G. Kouyoumjian and P. H. Pathak, "A uniform geometrical theory of diffraction for an edge in a perfectly conducting surface," *Proc. IEEE*, vol. 62, pp. 1448-1461, 1974.

[18] T. W. Veruttipong, "Time domain version of the uniform GTD," *IEEE Trans. Antennas Propagat.*, vol. 38, pp. 1757-1764, 1990.

[19] G. Gennarelli and G. Riccio, "Time domain diffraction by a right-angled penetrable wedge," *IEEE Trans. Antennas Propagat.*, vol. 60, pp. 2829-2833, 2012.

[20] G. Gennarelli and G. Riccio, "Obtuse-angled penetrable wedges: a time domain solution for the diffraction coefficients," *J. Electromagn. Waves Appl.*, vol. 27, pp. 2020-2028, 2013.

[21] M. Frongillo, G. Gennarelli, and G. Riccio, "TD-UAPO diffracted field evaluation for penetrable wedges with acute apex angle," *J. Opt. Soc. Am. A*, vol. 32, pp. 1271-1275, 2015.

[22] M. Frongillo, G. Gennarelli, G. Riccio, "Plane wave diffraction by co-planar adjacent blocks," in *Proc. 2016 LAPC*, Loughborough (UK).

[23] M. Frongillo, G. Gennarelli, and G. Riccio, "TD-UAPO solutions for the diffraction by co-planar adjacent blocks," in *Proc. 2017 Int. ACES Symp.*, Florence (Italy), 2017.

[24] G. Riccio, "Uniform Asymptotic Physical Optics solutions for a set of diffraction problems", in *Wave Propagation in Materials for Modern Applications*, A. Petrin Ed., Vukovar (HR): Intech, 2010, pp. 33-54.

[25] P. C. Clemmow, *The Plane Wave Spectrum Representation of Electromagnetics Fields*, ser. IEEE/OUP Series on Electromagnetics wave theory. Piscataway: IEEE, 1996.

[26] G. D. Maliuzhinets, "Inversion formula for the Sommerfeld integral," *Sov. Phys. Dokl*., vol. 3, pp. 52–56, 1958.

[27] A. Taflove and S. Hagness, *Computational Electrodynamics: The Finite Difference Time Domain Method*. Norwood: Artech House, 2000.